Perturbation of Dopamine Metabolism by 3-Amino-2-(4'-halophenyl)propenes Leads to Increased Oxidative Stress and Apoptotic SH-SY5Y Cell Death

Warren C. Samms, Rohan P. Perera, D. S. Wimalasena, and K. Wimalasena

Department of Chemistry, Wichita State University, Wichita, Kansas

ABSTRACT

We have recently characterized a series of 3-amino-2-phenyl-propene (APP) derivatives as reversible inhibitors for the bovine adrenal chromaffin granule vesicular monoamine transporter (VMAT) that have been previously characterized as potent irreversible dopamine-β-monooxygenase (DβM) and monoamine oxidase (MAO) inhibitors. Halogen substitution on the 4'-position of the aromatic ring gradually increases VMAT inhibition potency from 4'-F to 4'-I, parallel to the hydrophobicity of the halogen. We show that these derivatives are taken up into both neuronal and non-neuronal cells, and into resealed chromaffin granule ghosts efficiently through passive diffusion. Uptake rates increased according to the hydrophobicity of the 4'-substituent. More importantly, these derivatives are highly toxic to human neuroblastoma SH-SY5Y but not toxic to M-1, Hep G2, or human embryonic kidney 293 non-neuronal cells at similar concentrations. They drastically perturb dopamine (DA) uptake and metabolism in SH-SY5Y cells under sublethal conditions and are able to deplete both vesicular and cytosolic catecholamines in a manner similar to that of amphetamines. In addition, 4'-IAPP treatment significantly increases intracellular reactive oxygen species (ROS) and decreases glutathione (GSH) levels in SH-SY5Y cells, and cell death is significantly attenuated by the common antioxidants α-tocopherol, N-acetyl-L-cysteine and GSH, but not by the nonspecific caspase inhibitor N-benzyloxycarbonyl-Val-Ala-Asp-fluoromethyl ketone. DNA fragmentation analysis further supports that cell death is probably due to a caspase-independent ROS-mediated apoptotic pathway. Based on these and other findings, we propose that drastic perturbation of DA metabolism in SH-SY5Y cells by 4'-halo APP derivatives causes increased oxidative stress, leading to apoptotic cell death.

Oxidative stress in the central and peripheral nervous systems plays a significant role in neurodegenerative disorders, aging, and the toxicity of a large number of neurotoxins (Cadet and Brannock, 1998; Halliwell, 2006). Auto-oxidizable catecholamines dopamine (DA), NE, and E and their metabolites are known to generate H_2O_2, reactive oxygen species (ROS), and organic radicals under aerobic conditions because of their intrinsic redox properties (Hald and Lotharius, 2005; Ogawa et al., 2005). Therefore, catecholaminergic neurons

are inherently subjected to higher oxidative stress and more free radical damage than other types of neurons (Graham, 1978; Adams et al., 2001). Although most reactive radical species are effectively scavenged by enzymatic defense mechanisms and cellular antioxidants in vivo, excessive generation may lead to extensive cellular damage (Fridovich, 1986; Frei et al., 1989).

Numerous studies indicate that efficient uptake, biosynthetic conversion, and storage of catecholamines in vesicles are mandatory for proper functioning of catecholaminergic neurons. The vital proteins responsible, including vesicular H^+-ATPase (V-H^+-ATPase), cytochrome b_{561} (b_{561}), dopamine-β-monooxygenase (DβM), and vesicular monoamine transporter (VMAT), have been well characterized (Beers

ABBREVIATIONS: DA, dopamine; NE, norepinephrine; E, epinephrine; ROS, reactive oxygen species; b_{561}, cytochrome b_{561}; V-H^+, vesicular H^+; DβM, dopamine-β-monooxygenase; VMAT, vesicular monoamine transporter; Asc, ascorbic acid; DAT, dopamine transporter; MPP$^+$, 1-methyl-4-phenylpyridinium; APP, 3-amino-2-phenylpropene; OHAPP, hydroxy-3-amino-2-phenylpropene; MAO, monoamine oxidase; GSH, reduced glutathione; GBR 12909, vanoxerine; Z-VAD-FMK, N-benzyloxycarbonyl-Val-Ala-Asp-fluoromethyl ketone; FBS, fetal bovine serum; HPLC, high-performance liquid chromatography; HPLC-EC, HPLC with electrochemical detection; HPLC-UV, HPLC with UV detection; DMEM, Dulbecco's modified Eagle's medium; MTT, 3-(4,5-dimethylthiazol-2-yl)-2,5-diphenyltetrazolium bromide; NAC, N-acetyl-cysteine; KRB, Krebs-Ringer buffer; DOPAC, 3,4-dihydroxyphenylacetic acid; HVA, homovanillic acid; DCF-DA, 2',7'-dichlorofluorescein diacetate; DCF, 2',7'-dichlorofluorescein; MCB, monochlorobimane.

et al., 1986; Wakefield et al., 1986; Wimalasena and Wimalasena, 1995, 2004). V-H$^+$-ATPase generated transmembrane pH gradient is mandatory for the granular accumulation of catecholamines, as well as the regeneration of intragranular ascorbic acid (Asc) from semidehydroascorbate, through b$_{561}$. In addition to providing reducing equivalents to DβM reaction, a high concentration of intragranular Asc ensures a reductive environment, preserving catecholamines from auto-oxidation. Therefore, tightly coordinated, well integrated functions of V-H$^+$-ATPase, VMAT, DβM, and b$_{561}$ are not only necessary for efficient granular accumulation, storage, and biotransformation of catecholamines but also essential for relieving catecholamine-induced oxidative stress. Perturbation of catecholamine metabolism through impaired intragranular accumulation and biotransformation could lead to increased oxidative stress and eventual neurodegeneration.

In agreement with the above proposals, recent studies show that the neuropharmacological and neurotoxic effects of a large number of illicit drugs and neurotoxins are closely associated with interference of catecholamine storage and metabolism. For example, increasing evidence suggests that amphetamine-related drugs exert their effects by increasing the nonexocytotic release of dopamine in some regions of the brain (Di Chiara and Imperato, 1988; Sabol and Seiden, 1992) through direct interaction with plasma membrane dopamine transporter (DAT) and VMAT (Rudnick and Wall, 1992; Schuldiner et al., 1993; Riddle et al., 2005). In addition, the neurotoxicity of the Parkinsonian toxin 1-methyl-4-phenylpyridinium (MPP$^+$) is believed to be due, at least in part, to its ability to interfere with vesicular uptake/storage of DA in dopaminergic neurons (Daniels and Reinhard, 1988; Liu et al., 1992; Lotharius and O'Malley, 2000).

We have recently characterized a series of 3-amino-2-phenylpropene (APP) derivatives as novel reversible inhibitors for the bovine adrenal chromaffin granule VMAT (Perera et al., 2003), which have been previously characterized as irreversible DβM (May et al., 1983; Padgette et al., 1985) and MAO (McDonald et al., 1985) inhibitors. We have reported that VMAT inhibition potencies of 4′-halogenated APP derivatives were dependent on the 4′-substituent and increased in the order 4′-F < 4′-Cl < 4′-Br < 4′-I. In the present study, we demonstrate that whereas 4′-halogen-substituted APP derivatives are highly toxic to SH-SY5Y cells, they are not toxic to non-neuronal cell lines at similar concentrations, and cell toxicities of these derivatives parallel their relative VMAT inhibition potencies and hydrophobicities. These compounds are efficiently accumulated into both neuronal and non-neuronal cells and resealed chromaffin granule ghosts through simple diffusion, and uptake rates follow the same 4′-substituent dependence as SH-SY5Y toxicity. They drastically reduce DA uptake, storage, and metabolism and dissipate the catecholamine content in SH-SY5Y cells at low concentrations and short incubation times. Furthermore, 4′-IAPP treatment significantly increases intracellular ROS specifically in SH-SY5Y cells and also lowers reduced glutathione (GSH) levels. In addition, toxicity is attenuated by commonly used antioxidants. DNA fragmentation analysis and caspase inhibition studies suggest that cell death may involve a caspase-independent apoptotic pathway. Based on these and other findings, we propose that perturbation of DA metabolism by 4′-halo APP derivatives through VMAT, DβM, and/or MAO inhibition and granular accumulation in SH-SY5Y cells leads to increased oxidative stress and cell death. Our data support the proposal that proper storage of catecholamines in storage vesicles is not only vital for normal physiological functioning, but also necessary to protect catecholaminergic neurons from self-induced oxidative stress.

Materials and Methods

Reagents. Synthesis and characterization of all APP derivatives have been previously reported (Padgette et al., 1985; Perera et al., 2003). MPP$^+$I was synthesized as described by Das et al. (1993). APP derivatives (10 mM), GBR 12909 dihydrochloride (1 mM), and desipramine hydrochloride (1 mM) stock solutions were prepared in water, and rotenone (4 mM) stock solution was prepared in ethanol. Commercial α-tocopherol was diluted with EtOH to a 50 mM stock solution. The nonspecific caspase inhibitor Z-VAD-FMK (R&D Systems, Minneapolis, MN) was diluted to a 20 mM stock solution in dimethyl sulfoxide. All cell culture media and reagents were purchased from Sigma-Aldrich except FBS, which was purchased from Lonza Bioscience (Walkersville, MD). All other reagents (highest purity available) and laboratory supplies were purchased from either Thermo Fisher Scientific (Waltham, MA) or Sigma-Aldrich (St. Louis, MO).

Instrumentation. UV-visible spectra were recorded on a Cary Bio 300 UV-visible spectrophotometer (Varian, Inc., Palo Alto, CA). Fluorescence emission spectra were recorded using a Jobin Yvon-Spex τ-3 spectrofluorimeter (HORIBA Jobin Yvon, Inc., Edison, NJ). Analyses of catecholamines were carried out using reversed-phase HPLC with electrochemical detection (HPLC-EC) on a C$_{18}$ reversed-phase column as described previously (Wimalasena and Wimalasena, 1995, 2004). Reversed-phase HPLC with UV detection (HPLC-UV) analyses were performed on a Spectra System P4000 gradient pump equipped with a SCM 1000 vacuum degasser coupled to an LDC Analytical SM 4000 UV detector (all from Thermo Fisher Scientific, Waltham, MA) using a C$_{18}$ reversed-phase column (Supelco, Bellefonte, PA). Elution buffer consisted of a 50:15:35 ratio of 50 mM NaOAc, pH 4.5/CH$_3$CN/CH$_3$OH. Flow rate was 0.8 ml/min. Cell sonications were performed using two 2-s pulses from a Thermo Fisher Scientific Sonic Dismembrator model 100.

Cell Culture. SH-SY5Y cells were purchased from American Type Culture Collection (Manassas, VA); M-1 cells were obtained from Dr. Karyn Turla (Friends University, Wichita, KS), Hep G2 and HEK-293 cells were from Dr. Tom Wiese (Fort Hays State University, Hays, KS). SH-SY5Y human neuroblastoma cells, human embryonic kidney (HEK)-293 cells, and Hep G2 liver carcinoma cells were grown in high-glucose Dulbecco's modified Eagle's medium (DMEM) supplemented with 10% FBS at 37°C and 5% CO$_2$. M-1 murine renal tubule cells were cultured in 1:1 DMEM/Ham's F-12 media supplemented with 5% FBS, 5 μM dexamethasone, and 2.5 mM L-glutamine at 37°C and 5% CO$_2$. All cells were cultured in 100-mm^2 tissue culture plates until approximately 80% confluence and then seeded into multiwell plates, depending on the nature of the experiment. When EtOH or dimethyl sulfoxide was used as a cosolvent, final concentrations were kept at ≤0.1 or 1.0%, respectively.

Preparation of Chromaffin Granule Ghosts. Chromaffin granules and lysed granule membranes were prepared from fresh bovine adrenal medullae as described previously (Wimalasena and Wimalasena, 1995, 2004). Granule membranes were washed and resealed to contain 20 mM Tris-phosphate, 100 mM KCl, 150 mM sucrose, 10 mM sodium fumarate, 4.0 μM copper, 100 μg/ml catalase, and 20 mM Asc. The resealed ghosts were purified by a 15% Ficoll (GE Healthcare, Chalfont St. Giles, Buckinghamshire, UK), 0.3 M sucrose, and 10 mM HEPES, pH 7.0, discontinuous density gradient as described previously (Wimalasena and Wimalasena, 1995, 2004).

Cell Viability. Cell viability was measured using the 3-(4,5-dimethylthiazol-2-yl)-2,5-diphenyltetrazolium bromide (MTT) assay (Denizot and Lang, 1986). In brief, cells were seeded into 96-well plates at 5×10^4 cells/well and grown 1 to 2 days to achieve ~80% confluence. Cells were treated with the desired concentration of 4′-halo APP derivatives (0–1000 μM) in a total volume of 50 μl of phenol red-free complete DMEM for 24 h. After the incubation period, 20 μl of 5 mg/ml MTT solution was added to each well and was incubated for 2 h at 37°C. The resulting formazan was solubilized by addition of 200 μl of detergent solution (50% dimethylformamide, 20% SDS) followed by incubation for 12 h at 37°C. Cell viability was determined by quantifying the formazan, based on the difference in the absorbance at 570 and 650 nm. Results are expressed as percentage of APP untreated control cells.

Neuroprotective Studies. SH-SY5Y cells were grown in 96-well plates as described above and were incubated with various concentrations of either α-tocopherol (0–25 μM), *N*-acetyl-cysteine (NAC; 0–25 μM), or GSH (0–25 μM) in DMEM for 2 h. Then, 200 μM 4′-IAPP (final concentration) was added and cells were incubated for 24 h, and cell viability was determined by the MTT assay as described above. Results are expressed as percentage of APP-untreated control subjects. The effects of the inhibition of caspases on cell viability was evaluated using the nonspecific caspase inhibitor Z-VAD-FMK (0–25 μM in DMEM) using the same procedure described above for antioxidants. Results are expressed as percentage of APP-untreated control subjects.

Cellular Uptake. Uptake of 4′-halo APP derivatives into SH-SY5Y or HEK-293 cells was determined by reversed-phase HPLC-UV. Cells were seeded into six-well plates at 1×10^6 cells/well and grown 1 to 2 days to achieve ~80% confluence. The media was removed, and a solution containing 50 μM 4′-halo APP derivative in warm Krebs-Ringer buffer (KRB; 125 mM NaCl, 2 mM KCl, 1.4 mM $MgSO_4$, 1.2 mM $CaCl_2$, 1.2 mM KH_2PO_4, 20 mM HEPES, and 5 mM glucose, pH 7.4) was added to each well and incubated for 0 and 30 min at 37°C, at which time the media was removed and cells were washed three times with ice-cold KRB. Washed cells were transferred into a 1.5-ml microcentrifuge tube and centrifuged at 500g for 5 min. The supernatant was discarded and the cell pellet was treated with 100 μl of 0.1 M $HClO_4$. The coagulated proteins were pelleted by centrifugation at 15,000g for 5 min at 4°C, and the concentration of each 4′-halo APP in acidic supernatants was determined by reversed-phase HPLC-UV analysis as detailed above. All 4′-halo APP levels were normalized to the respective protein concentrations, and the readings were corrected for nonspecific binding by subtracting the corresponding time 0-point readings from the 30-min readings.

Granular Uptake. The ghosts prepared as described above were suspended in a medium containing 0.3 M sucrose, 10 mM HEPES, pH 7.0, 5 mM $MgSO_4$, 100 μg/ml catalase, 5 mM ATP, and 5 mM Asc in a total volume of 1.75 ml. This mixture was preincubated for 10 min at 30°C and reactions were initiated by the addition of a 100 μM concentration of the desired 4′-halo APP derivative. Aliquots (400 μl) of the incubate were withdrawn at 0-, 15-, 30-, and 45-min time intervals, diluted into 5.0 ml of ice-cold 0.4 M sucrose and stored on ice until the end of the experiment. Finally, ghosts were reisolated from these samples washed as previously reported (Wimalasena and Wimalasena, 1995, 2004), lysed with 0.1 M $HClO_4$, and intragranular 4′-halo APP concentrations were determined by HPLC-UV as detailed above. All 4′-halo APP levels were normalized to the respective granule protein concentrations, and the readings were corrected for nonspecific binding by subtracting the corresponding time 0 readings from the other time point readings.

Catecholamine Perturbation. SH-SY5Y cells were seeded into 12-well plates at 0.5×10^6 cells/well and grown to near confluence before experimentation. Cells were incubated with 40 μM each 4′-halo APP derivative in KRB for 10 min at 37°C. DA was then added to the medium to a final concentration of 50 μM, and samples were incubated an additional 30 min at 37°C. Cells were washed three times with ice-cold KRB and harvested as detailed above, and intra-

cellular DA, NE, DOPAC, and HVA levels were quantified by reversed-phase HPLC-EC analysis as detailed above. In a second set of experiments, SH-SY5Y cells were initially incubated with 50 μM DA for 30 min and washed with KRB followed by incubation with 40 μM 4′-IAPP in KRB for 30 min. Cells were washed and harvested, and catecholamine levels were quantified. Catecholamine levels were normalized to the total protein content of each sample and compared with parallel untreated control samples.

Reactive Oxygen Species. Intracellular ROS levels were quantified by using the 2′,7′-dichlorofluorescein diacetate (DCF-DA) method (Oubrahim et al., 2001). In brief, SH-SY5Y or HEK-293 cells were seeded into six-well plates at 1×10^6 cells/well and grown for 1 to 2 days in complete DMEM to near-confluence. Cells were treated with desired concentrations of 4′-IAPP for 1 h followed by addition of 50 μM DCF-DA for 1 h. Cells were washed, harvested, and lysed with 0.1 M Tris buffer, pH 7.5, containing 1% Triton X-100, and the DCF fluorescence of supernatants were measured (excitation at 504 nm; emission at 526 nm) after removal of cellular debris by centrifugation at 15,000g for 5 min at 37°C. Fluorescence readings were normalized to the total protein content of respective samples using the bicinchoninic acid method (Smith et al., 1985).

Intracellular Reduced Glutathione. Intracellular reduced glutathione levels were measured using the monochlorobimane (MCB)-based fluorescence assay (Nair et al., 1991). SH-SY5Y cells were grown in 12-well plates and treated with various concentrations of 4′-IAPP in complete DMEM for 24 h. MCB was then added to a final concentration of 40 μM in each well and further incubated for 30 min. Cells were washed and suspended in 1 ml of Ca^{2+}/Mg^{2+}-free PBS, transferred into 1.5-ml microcentrifuge tubes, and sonicated. The characteristic fluorescence of the reduced glutathione adduct of bimane was measured and quantified (excitation at 390 nm/emission at 478 nm). Fluorescence readings were normalized to the total protein content of each sample.

Apoptotic DNA Laddering. SH-SY5Y cells were cultured in 60-mm^2 plates (5×10^6 cells/plate) for 24 h and treated with 0, 100, or 300 μM 4′-IAPP or 4 μM rotenone for 24 h. Total cellular DNA was extracted using the DNeasy DNA Isolation Kit (QIAGEN, Valencia, CA) according to the manufacturer's instructions, including treatment with proteinase K and RNase A. DNA samples were loaded onto a 1.2% agarose gel and electrophoresed at 70 V for 2 to 3 h until the bromphenol blue band had migrated approximately two thirds of the way down the gel. DNA bands were stained with ethidium bromide, visualized on a UV transilluminator, and photographed using a Kodak Gel Logic 100 system (Eastman Kodak, Rochester, NY). Cells treated with 4 μM rotenone were included as a positive control for ROS-induced apoptotic cell death (Watabe and Nakaki, 2004).

Protein Quantification. Protein quantifications were generally carried out by the Bradford method (Bradford, 1976), except in ROS analysis experiments, where the protein was determined by the bicinchoninic acid method as a result of the presence of 1% Triton X-100 in the samples (Smith et al., 1985).

Data Analysis. All results represent the mean of at least three experimental trials. Error bars represent the sample S.D., and significance was tested by either two-tailed Student's t test or one-way analysis of variance. Values of $p < 0.05$ were considered statistically significant. When applicable, quantitative experimental data were normalized to the protein content of each sample.

Technical Statement. Due to the potentially unclear mode of action and seemingly nonspecific mode of cellular entry, extreme caution was used when using the compounds discussed in this article in accordance with published precautions of related neurotoxins (Przedborski et al., 2001).

Results

As summarized in Table 1, we have shown previously that APP derivatives are novel inhibitors for bovine chromaffin

granule VMAT (Perera et al., 2003). These studies have also shown that 4′-OHAPP, a structural analog of the VMAT substrate tyramine, behaves as a competitive inhibitor for VMAT having an affinity similar to that of DA. In addition, data in Table 1 show that 4′-halogen substitution increases the VMAT inhibition potency from -F to -I, parallel to their overall hydrophobicities. Previous studies have shown that APP derivatives possess potent irreversible inhibition properties toward MAO (McDonald et al., 1985) and DβM (Padgette et al., 1985). The structural similarities, gradually increasing VMAT inhibition potencies and hydrophobicities within the series of 4′-halogen substitutes APP derivatives make them a unique series of probes that can be used to examine the effects of the perturbation of DA metabolism in catecholaminergic neurons.

Cellular uptake of 4′-halo APP derivatives was examined using a series of short-time incubations employing low concentrations. In these experiments, SH-SH5Y cells were incubated with each 4′-halo APP derivative and the intracellular APP concentrations were quantified by HPLC-UV as detailed under *Materials and Methods*. The zero time points were used to determine the degree of nonspecific binding of each derivative and were subtracted from the 30-min readings to accurately determine the intracellular concentrations. As shown in Fig. 1, 4′-ClAPP, 4′-BrAPP, and 4′-IAPP were effectively taken up into SH-SY5Y cells, whereas uptake of 4′-FAPP is considerably lower. Furthermore, the relative uptake of these derivatives were both time- and concentration-dependent and not significantly altered by the presence of 1 μM DAT or NET inhibitors—GBR 12909 or desipramine, respectively (data not shown). These derivatives were also taken up into non-neuronal HEK-293 cells in a concentration- and time-dependent manner, with rates similar to that of SH-SY5Y cells (data not shown).

We previously reported that 3′- and 4′-OHAPP derivatives are not taken into resealed chromaffin granule ghosts at a detectable rate (Padgette et al., 1985; Perera et al., 2003). However, as 4′-halo APP derivatives are significantly more hydrophobic and are freely taken up by SH-SY5Y and other cells; we expected that these derivatives may also be taken up into chromaffin granule ghosts through simple diffusion. To test this possibility, a series of standard uptake experiments were carried out with resealed chromaffin granule ghosts and the above APP derivatives. The data in Fig. 2 show that whereas 4′-I and 4′-BrAPP derivatives were taken up effectively, 4′-ClAPP was taken up relatively slowly. Similar to cellular uptake, 4′-FAPP uptake was low and could not be accurately quantified under the experimental conditions.

Initial screening experiments have revealed that only certain APP derivatives are highly toxic to human neuroblastoma SH-SY5Y cells. It is noteworthy that whereas the 4′-halogenated derivatives were found to be the most toxic, the more polar 3′- and 4′-OH derivatives, with VMAT inhibition potencies comparable with those of 4′-halo derivatives, were found to have no apparent toxicity to these cells (data not shown). Based on these observations, 4′-halo APP derivatives were chosen as the best candidates for detailed toxicological and structure-activity studies. As seen in Fig. 3A, these derivatives induce marked concentration-dependent cellular death in SH-SY5Y cells over a 24-h incubation period. The estimated LC$_{50}$ values range from 867 μM for 4′-FAPP to 204 μM for 4′-IAPP. Comparative toxicity experiments with MPP$^+$, which has been extensively used as a model dopaminergic neurotoxin (Burns et al., 1983; Song et al., 1997; Lotharius and O'Malley, 2000), have shown that the 4′-halo APP derivatives are significantly more toxic than MPP$^+$ to SH-SY5Y cells, under similar experimental conditions. Exposure of SH-SY5Y cells to 1000 μM MPP$^+$ for 24 h reduces cell viability to ~75%, which is equivalent to the effect of 100 μM 4′-IAPP treatment for the same time period. Data pre-
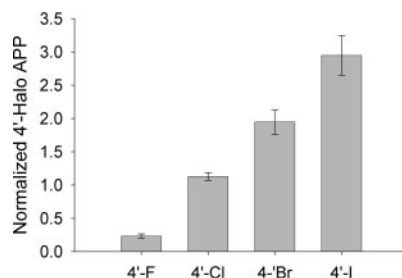

Fig. 1. Uptake of 4′-halo APP into SH-SY5Y cells. Cells were grown in six-well plates and were incubated with the desired 4′-halo APP derivative (50 μM) in KRB for 30 min. Media was removed and cells were washed three times with ice-cold KRB. The intracellular 4′-halo APP concentrations were determined by reversed-phase HPLC-UV and were normalized to respective cellular protein concentrations. All readings were corrected for nonspecific binding by subtracting the corresponding $t = 0$ readings. Data represent mean ± S.D. of triplicate samples and are statistically different based on one-way analysis of variance analysis ($p < 0.001$).
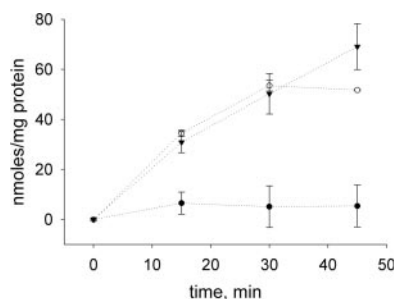

Fig. 2. Uptake of 4′-halo APP into resealed chromaffin granule ghosts. Resealed chromaffin granule ghosts prepared as detailed under *Materials and Methods* were suspended in a medium containing 0.3 M sucrose, 10 mM HEPES, pH 7.0, 5 mM ATP, 5 mM MgSO$_4$, 100 μg/ml catalase, and 5 mM Asc. This mixture was preincubated for 10 min at 30°C and reactions were initiated by addition of a 100 μM concentration of the desired 4′-halo APP derivative. Aliquots (400 μl) of the incubate were withdrawn at 0-, 15-, 30-, and 45-min time intervals, and intragranular levels of 4′-halo APP derivatives were quantified by HPLC-UV and were normalized to respective granule protein concentrations. The intragranular concentration of 4′-FAPP was low and could not be quantified accurately because of sensitivity limitations of HPLC-UV. All readings were corrected for nonspecific binding by subtracting the corresponding t = 0 readings. Data represent mean ± S.D. of triplicate samples. ●, 4′-ClAPP; ○, 4′-BrAPP; ▼, 4′-IAPP.

TABLE 1

DA uptake inhibition in resealed bovine chromaffin granules

Data from Perera et al. (2003). The nonstandard $K_{m, DA}/K_i$ ratios were calculated from the respective K_i and $K_{m, DA}$ parameters determined for each compound to normalize the variation of K_m for DA for different ghost preparations. These values also provide a measure of their relative abilities to compete with DA under the same experimental conditions.

	$K_i \pm$ S.D.	$K_{m, DA}/K_i$
	μM	
4′-OHAPP	15.5 ± 0.9	1.52
3′-OHAPP	16.7 ± 1.1	1.40
4′-FAPP	42.3 ± 3.1	0.80
4′-ClAPP	18.0 ± 0.9	1.76
4′-BrAPP	17.7 ± 2.0	1.79
4′-IAPP	12.9 ± 2.3	2.96

sented in Fig. 3B further demonstrates that 4′-IAPP mediated SH-SY5Y cell death is time-dependent. At 400 μM, 4′-IAPP-induced cell death was quite rapid with greater than 50% cell death occurring within the initial 3 h, and after 24 h, no viable cells could be detected.

To determine the specificity of the observed toxicity of 4′-halo APP derivatives, 4′-IAPP was evaluated against several commonly used non-neuronal cell lines (Hep G2, HEK-293, and M-1). As shown in Fig. 3C, 4′-IAPP is not toxic to any of these cell lines in the concentration range tested (0–400 μM). Whereas both Hep G2 and HEK-293 cells maintain 100% viability throughout this concentration range, interestingly, M-1 cells seem to show a concentration-dependent stimulation of cell growth with respect to a parallel control. However, at 4′-IAPP concentrations above 500 μM,
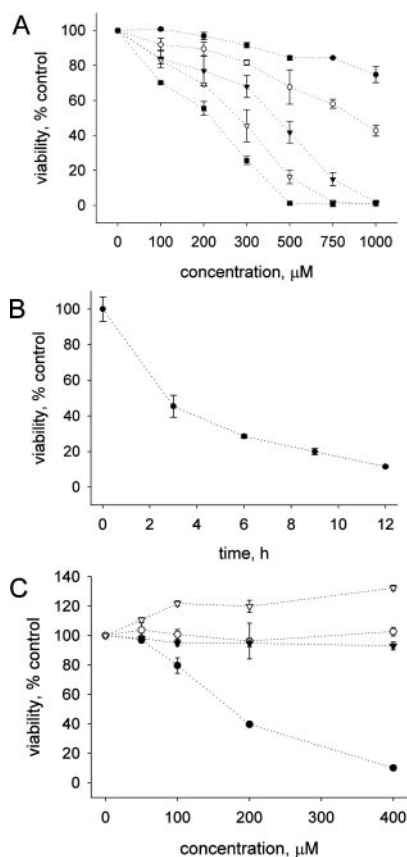

Fig. 3. 4′-Halo APP toxicity is both concentration- and time-dependent, and specific for SH-SY5Y cells. A, SH-SY5Y cells grown in 96-well plates were treated with 0 to 1000 μM 4′-halo APP derivatives in phenol-red free complete DMEM for 24 h, and cell viability was determined by the MTT assay as detailed under *Materials and Methods*. The classic neurotoxin MPP$^+$ was included for comparative purposes. Data represent mean ± S.D. of at least six separate experiments carried out in triplicate sets. ●, MPP$^+$; ○, 4′-FAPP; ▼, 4′-ClAPP; ▽, 4′-BrAPP; and ■, 4′-IAPP. B, SH-SY5Y cells grown as in A were treated with 400 μM 4′-IAPP in phenol-red free complete DMEM for the various time intervals (0–12 h), and cell viability was measured using the MTT assay. Data represent mean ± S.D. of at least six separate experiments carried out in triplicate sets. C, SH-SY5Y, HEK-293, Hep G2, and M-1 cells were grown in 96-well plates and treated with various concentrations of 4′-IAPP (0–400 μM) in complete medium for 24 h, and cell viabilities were determined by MTT assay. At higher 4′-IAPP concentrations (>500 μM), some nonspecific cell death was observed in HEK-293 and Hep G2 cells but not in M-1 (data not shown). Data represent mean ± S.D. of at least six separate experiments carried out in triplicate sets. ●, SH-SY5Y cells; ○, HEK-293 cells; ▼, Hep G2 cells; ▽, M-1 cells

some modest cellular toxicity has been observed in HEK-293 and Hep G2 cells.

As shown in Fig. 3B, SH-SY5Y cell death induced by 4′-IAPP was quite rapid. In addition, the cellular toxicities of these derivatives are also associated with rapid morphological changes. Morphological changes associated with 45-min 4′-IAPP (100 or 300 μM) treatment is shown in Fig. 4. The normal oblong, extended appearance of SH-SY5Y cells (Fig. 4A) was altered to a shrunken spherical appearance after 300 μM 4′-IAPP treatment (Fig. 4C). Cells treated with 100 μM 4′-IAPP show only modest morphological changes at 45 min (Fig. 4B), but became increasingly apparent at longer exposure times (data not shown). On the other hand, similar treatments of HEK-293 and Hep G2 cells with 4′-IAPP show no significant morphological changes, consistent with observed resistance of these cells to 4′-IAPP toxicity.

We have reported previously that APP derivatives effectively interfere with the accumulation of DA in resealed chromaffin granule ghosts (Perera et al., 2003). Current studies using resealed granule ghosts (Fig. 2) show that that 4′-halo APP derivatives may effectively accumulate in storage vesicles, further perturbing the DA metabolism. Thus, a series of experiments was performed to evaluate the ability of 4′-halo APP derivatives to interfere with DA uptake and storage. SH-SY5Y cells were initially incubated with a 40 μM concentration of the desired 4′-halo APP derivative for 10 min followed by 50 μM DA for 30 min as described under *Materials and Methods* to evaluate the degree of DA uptake impairment. Data in Fig. 5A demonstrate that 4′-halo APP pretreatment drastically reduces intracellular catecholamine levels (DA, NE, DOPAC, and HVA) and the extent of these effects were in the order 4′-IAPP > 4′-BrAPP > 4′-ClAPP > 4′-FAPP. Likewise, catecholamine levels in cells preloaded with exogenous DA by incubating SH-SY5Y cells with 50 μM DA for 30 min are also significantly depleted by the incubation with 100 μM 4′-IAPP in KRB for 50 min (Fig. 5B). However, catecholamine depletion under these conditions was somewhat slower, requiring higher concentrations of 4′-halo APP and longer incubation times to obtain comparable reductions. Although all four 4′-halo APP derivatives were investigated, only the results of 4′FAPP and 4′IAPP are displayed in Fig. 5 for purposes of clarity. In almost all experimental trials, the degree of catecholamine depletion induced by 4′ClAPP and 4′BrAPP was between that of 4′FAPP and 4′IAPP.

The ROS levels of 4′I-APP treated SH-SY5Y and HEK-293 cells were measured using standard techniques as detailed under *Materials and Methods*. As shown in Fig. 6, treatment of SH-SY5Y cells with 4′-IAPP (50 and 150 μM) for 1 h results in a rapid increase of intracellular ROS levels by approximately 20 and 40% respectively, compared with an untreated control cell. On the other hand, treatment of HEK-293 cells under the same conditions does not result in increased intracellular ROS levels, suggesting that 4′-IAPP-induced increased ROS production is specific to SH-SY5Y cells.

Data presented Fig. 7 show that the commonly used antioxidant NAC significantly attenuates cell death in a concentration-dependent manner. For example, preincubation of cells with 25 μM NAC for 2 h followed by 200 μM 4′-IAPP treatment for 24 h increased viability by ~20%, compared with an untreated control. Similar experiments with GSH

showed that it is somewhat less effective but still showed a statistically significant increase in cell viability by ~15% (data not shown). It is noteworthy that α-tocopherol pretreatment provides the most protection of the antioxidants studied, increasing cell viability by ~30% at 25 μM, under similar conditions, compared with untreated control cells (data not shown). The effect of the nonspecific caspase inhibitor Z-VAD-FMK was used to evaluate whether a caspase-mediated apoptotic cell death pathway is involved in 4′-IAPP-induced SH-SY5Y cell death. These experiments have revealed that concentrations of Z-VAD-FMK up to 25 μM were not effective in protecting cells from 200 μM 4′-IAPP-induced SH-SY5Y cell death (data not shown).

To determine the effect of increased ROS production on the overall antioxidant balance of SH-SY5Y cells, intracellular GSH levels were fluorometrically determined as described under *Materials and Methods*. Upon 24-h exposure of SH-SY5Y cells to 25, 50, and 100 μM 4′-IAPP, intracellular GSH levels were found to be significantly decreased in a concentration-dependent manner compared with untreated control (Fig. 8).

4′-IAPP treated SH-SY5Y cells were examined for internucleosomal DNA cleavage—a marker of apoptotic activity. As seen in Fig. 9, agarose gel electrophoresis of nuclear DNA isolated from 300 μM 4′-IAPP-treated SH-SY5Y cells shows a distinct fragmentation pattern (lane 3) in multiples of 200 bp, similar to that induced by the standard apoptotic agent rotenone (4 μM, lane 4). Background smearing visible in the control sample (Fig. 9, lane 1) and other lanes is due to a population of dead cells present in the samples before the beginning of the experiment. However, the apoptotic laddering pattern is distinctly present in Fig. 9, lanes 3 and 4, compared with the control, indicative of apoptotic activity.

Discussion

Cellular uptake of 4′-halo APP derivatives is dependent on the nature of the 4′-substituent and increases parallel to substituent hydrophobicity (Fig. 1). The observation that uptake into SH-SY5Y cells is not inhibited by the presence of DAT or NET inhibitors, and comparable rates of accumulation into non-neuronal and SH-SY5Y cells suggests that cellular uptake probably occurs through simple diffusion. Parallel studies have shown that 4′-halo APP derivatives are also efficiently accumulated into resealed granule ghosts in a time-dependent (Fig. 2) and concentration-dependent (data not shown) manner. The efficiency of granular accumulation follows a trend similar to that of cellular uptake, where rates increased according to the hydrophobicity of the molecule (4′-F < 4′-Cl ≪ 4′-Br ~ 4′-I). In contrast to the behavior of 4′-halo APP derivatives, more polar 4′-OHAPP and 3′-OHAPP were not taken up into cells or granule ghosts in detectable amounts as reported previously (Perera et al., 2003). This evidence further confirms that both cellular and granular uptake of 4′-halo APP derivatives must occur through simple diffusion as a result of their high hydrophobicities.

Among APP derivatives tested, 4′-halogen-substituted derivatives are the most toxic to SH-SY5Y cells, and toxicity parallels both cellular and granular uptake efficiencies (Fig. 3A). In addition, 4′-IAPP is significantly more toxic to SH-SY5Y cells than the well-characterized dopaminergic neurotoxin MPP$^+$ under identical experimental conditions. Toxicities are concentration- and time-dependent and gradually increasing from 4′-F (EC$_{50}$ = 867 μM) to 4′-I (EC$_{50}$ = 204 μM) (Fig. 3B). In contrast, they are not significantly toxic to non-neuronal cells. Likewise, 4′-OH and 3′-OHAPP derivatives are nontoxic to both SH-SY5Y and non-neuronal cells under similar experimental conditions.

We have previously shown that ring-substituted APP derivatives are good competitive inhibitors for chromaffin granule VMAT with respect to DA. Among APP derivatives tested, 4′-OH, 3′-OH, and 4′-halo derivatives are the most potent (Perera et al., 2003). Previous studies have shown that APP derivatives are also potent turnover-dependent, irreversible inhibitors for DβM (May et al., 1983; Padgette et al., 1985) and MAO (McDonald et al., 1985). Thus, the specific toxicity of 4′-halo derivatives to SH-SY5Y cells could be associated with a combination of factors that are not present in non-neuronal cells, including efficient and nonspecific passage into cells and storage vesicles, reversible inhibition of VMAT and/or irreversible inhibition of DβM and MAO leading to perturbation of catecholamine metabolism. Strong further support for this proposal could be derived from the observation that pretreatment of SH-SY5Y cells with sublethal concentrations of 4′-halo APP derivatives for short time periods drastically reduces DA uptake, conversion, and metabolism (Fig. 5A). Likewise, experiments in which SH-SY5Y cells were first loaded with exogenous DA [SH-SY5Y cells contain low levels of endogenous DA (I. Balasooriya and K. Wimalasena, unpublished observation)] further show that 4′-halo APP derivatives are capable of depleting preaccumulated intracellular catecholamines (Fig. 5B) similar to that reported after reserpine treatment (Rudnick, 1997). In addition, both experiments show that the catecholamine-depleting potency of 4′-halo APP derivatives parallel their cellular toxicities, cellular/granular uptake efficiencies, and VMAT inhibition potencies. However, we note that the effects of 4′ halo APP on intracellular catecholamine levels under uptake conditions (Fig. 5A) were more drastic than under DA-preloaded conditions (Fig. 5B). A potential explanation for this
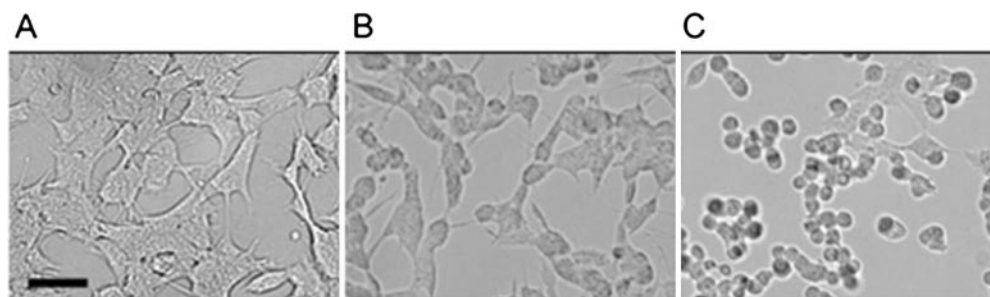

Fig. 4. Morphological changes of 4′-IAPP-treated SH-SY5Y cells. SH-SY5Y cells were grown in 60-mm² culture plates for 24 h and treated with 0, 100, or 300 μM 4′-IAPP. After 45 min of incubation, cells were photographed under phase-contrast microscopy at 100× magnification. A, untreated cells. B, cells treated with 100 μM 4′-IAPP. C, cells treated with 300 μM 4′-IAPP. Scale bar, 50 μm.

observation could be that these compounds, in addition to the perturbation of intracellular catecholamines, may also inhibit the uptake of extracellular DA, similar to that was observed with amphetamine and related compounds (Schuldiner et al., 1993; Kahlig et al., 2006). However, additional studies are certainly necessary to confirm this proposal firmly.

The toxicities of 4′-halo APP derivatives are associated with rapid morphological changes (Fig. 4), which are com-

Fig. 5. Effect of 4′-IAPP on catecholamine metabolism in SH-SY5Y cells. A, cells were grown in 12-well plates and incubated with 40 μM concentrations of each 4′-halo APP derivative in KRB for 10 min at 37°C. DA was then added to a final concentration of 50 μM, and samples were further incubated for 30 min at 37°C. Cells were washed and harvested, and intracellular DA, NE, DOPAC, and HVA levels were quantified by reversed-phase HPLC-EC analysis and normalized to respective cellular protein concentrations. Catecholamine levels are expressed as percentage of control DA levels (100%). Data represent mean ± S.D. of four samples. B, cells were grown in 12-well plates and incubated with 50 μM DA for 30 min, washed once with ice-cold KRB, and then incubated with 100 μM 4′-IAPP in KRB for 50 min. After incubation, cells were washed and harvested, and catecholamine levels were quantified by reversed-phase HPLC-EC analysis and normalized to respective cellular protein concentrations. Catecholamine levels are expressed as percentage of control DA levels (100%). Data represent ± S.D. of four samples. ∗, $p < 0.05$; ∗∗, $p < 0.01$; ∗∗∗, $p < 0.001$.
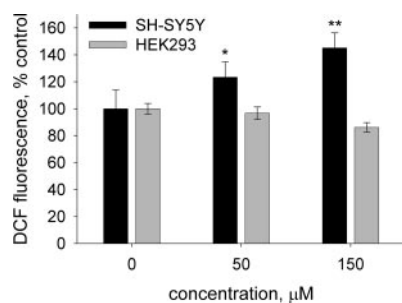
Fig. 6. Effect of 4′-IAPP on intracellular ROS levels. Intracellular ROS levels were quantified by the 2′,7′-dichlorofluorescein diacetate method (Oubrahim et al., 2001). SH-SY5Y and HEK-293 cells were incubated with various concentrations of 4′-IAPP in complete DMEM for 1 h; then the media was removed and 50 μM DCF-DA was added, and cells were incubated for an additional 1 h. Cells were washed and lysed, and DCF fluorescence was measured (excitation, 504 nm; emission, 526 nm) and normalized to respective cellular protein concentrations. Data represent mean ± S.D. of at least triplicate samples. ∗, $p < 0.05$; ∗∗, $p < 0.01$ compared with untreated control cells.

monly associated with apoptotic cell death (Mattson, 2006). Thus, the rapid onset of effects on SH-SY5Y cells observed in time course studies is consistent with the loss of cell viability through an apoptotic pathway. Strong support for this proposal is provided by the DNA laddering experiments, where characteristic 200-bp DNA fragmentation patterns were observed in 4′-IAPP-treated SH-SY5Y cells (Fig. 9). Such apoptotic processes may be initiated by a catecholamine-induced oxidative stress, because cellular toxicity of 4′-IAPP seems to be associated with the perturbation of catecholamine metabolism, as argued above. This notion is further supported the observation that 4′-IAPP induced rapid morphological changes correlate well with time frames of catecholamine perturbation as well as generation of excessive intracellular ROS. The exposure of SH-SY5Y cells to moderate 4′-IAPP concentrations show significant depletion of intracellular catecholamine levels and a simultaneous substantial increase in ROS levels (Fig. 6). In addition, treatment of HEK-293 cells under similar conditions resulted in no ROS increase, further suggesting that these effects are associated with 4′-IAPP-mediated perturbation of catecholamine metabolism in SH-SY5Y cells. Consistent with prolonged, excessive ROS production, 4′-IAPP induced a significant depletion in GSH
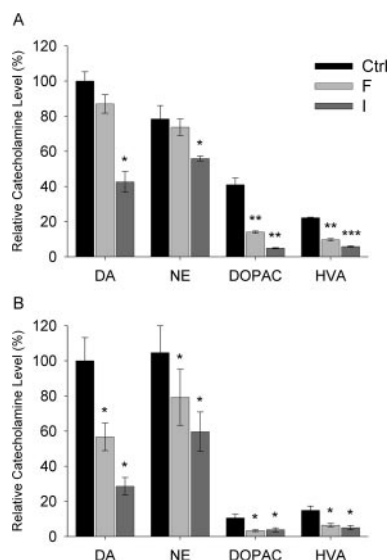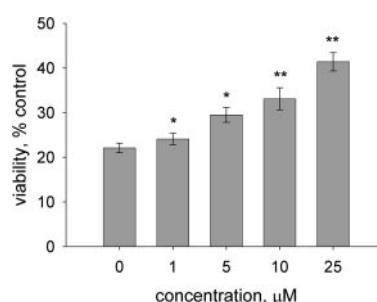

Fig. 7. Neuroprotective effect of NAC. SH-SY5Y cells were seeded into 96-well plates as described under Materials and Methods and incubated for 2 h with 0 to 25 μM NAC in phenol-red free DMEM, at which time 4′-IAPP was added to a final concentration of 200 μM in each well. Cells were incubated for 24 h, and viabilities were measured by MTT assay. We note that toxicity of 200 μM 4′-IAPP was slightly higher in this experiment compared with the data in Fig. 3, probably as a result of slight differences in experimental conditions and number of cell passages. Data represent mean ± of five samples. ∗, $p < 0.05$; ∗∗, $p < 0.01$ compared with unprotected control.
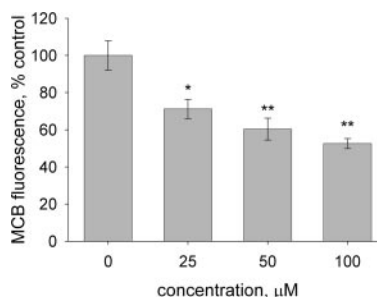

Fig. 8. Effect of 4′-IAPP on intracellular GSH levels. Intracellular reduced glutathione levels were measured using the MCB-based fluorometric assay (Nair et al., 1991). SH-SY5Y cells were grown in 12-well plates and treated with various concentrations of 4′-IAPP in complete DMEM for 24 h. Then, 40 μM MCB was added to each well, and cells were incubated for an additional 30 min. Cells were washed and lysed, and the characteristic fluorescence of the GSH-bimane adduct was quantified (excitation, 390 nm; emission, 478 nm) and normalized to respective cellular protein concentrations. Data represent mean ± S.D. of at least triplicate samples. ∗, $p < 0.05$; ∗∗, $p < 0.01$ compared with untreated control.
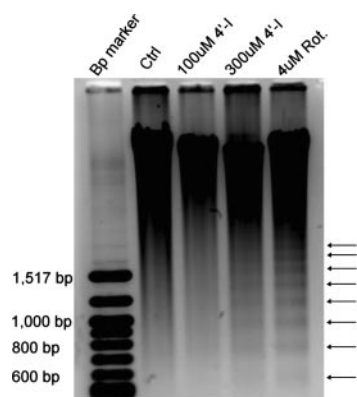
Fig. 9. 4′-IAPP induces apoptotic DNA laddering in SH-SY5Y cells. Cells were incubated for 24 h with either 4′I-APP [0 μM (lane 1), 100 μM (lane 2), 300 μM (lane 3)] or rotenone [4 μM (lane 4)]. DNA from treated cells was recovered using the QIAGEN DNeasy DNA Isolation Kit and was electrophoresed on a 1.2% agarose gel. The image was cropped and inverted from the original, with DNA marker bands representing 1517, 1200, 1000, 900, 800, and 700 bp. Both 300 μM 4′-IAPP and 4 μM rotenone show characteristic apoptotic 200-bp laddering, whereas control and 100 μM 4′-IAPP lanes do not.

levels in SH-SY5Y cells at longer incubation times (Fig. 8). These findings were further confirmed by the observation that commonly used antioxidants NAC, GSH, and α-tocopherol (25 μM) were found be effective in protecting SH-SY5Y cells from 4′-IAPP-induced cell death (Fig. 7). However, studies with the nonspecific caspase inhibitor Z-VAD-FMK suggest that the cell death is not due to a caspase-mediated pathway. These findings support the conclusion that 4′-halo APP-mediated SH-SY5Y cell toxicity may be due to oxidative stress-induced caspase-independent apoptotic cell death caused by excessive perturbation of catecholamine metabolism in SH-SY5Y cells.

Taken together, the above findings that 4′-halo APP derivatives are accumulated into both neuronal and non-neuronal cells but are specifically toxic to SH-SY5Y cells suggest that specific characteristics present in these cells, but absent in non-neuronal cells, are responsible for 4′-halo APP-induced toxicity. In addition, as mentioned above, these derivatives act as potent reversible VMAT and irreversible DβM and MAO inhibitors and are also efficiently accumulated into catecholamine storage vesicles. Thus, they should perturb DA uptake, storage, and metabolism similar to that of amphetamines (Kahlig et al., 2005). This notion is strongly supported by the observation that treatment with 4′-IAPP under sublethal conditions drastically reduced DA uptake, storage, and metabolism, and the extent of these effects parallel their toxicities. Thus, drastic, prolonged perturbation of DA storage and metabolism resulting in high oxidative stress is the most likely cause of 4′-halo APP toxicity specifically to SH-SY5Y cells. However, additional experimental data are certainly necessary to firmly establish the precise mechanism(s) of 4′-halo APP toxicity to these cells, in that it is not yet clear whether exclusive VMAT, DβM, or MAO inhibition, or a combination thereof, is primarily responsible for the observed catecholamine perturbation and neurotoxicity.

The intragranular environment is equipped to protect catecholamines from auto-oxidation by employing an acidic milieu, a high concentration of Asc, and low levels of redox-active materials, including transition metals. In contrast, cytosolic or extracellular conditions may favor the auto-oxi-

dation of catecholamines as a result of neutral pH (7.4), low Asc concentration, and the presence of various redox active materials. Auto-oxidation of catecholamines is known to produce reactive harmful radicals and increased oxidative stress (Tse et al., 1976; Sulzer et al., 2000; Ogawa et al., 2005). Thus, proper storage and metabolism of catecholamines in storage vesicles is not only vital for normal physiological functioning but also to protect cells from self-induced oxidative stress.

References

Adams JD Jr, Chang ML, and Klaidman L (2001) Parkinson's disease–redox mechanisms. *Curr Med Chem* **8:**809–814.

Beers MF, Johnson RG, and Scarpa A (1986) Reducing equivalents across chromaffin granule membrane. *J Biol Chem* **261:**2529–2535.

Bradford MM (1976) A rapid and sensitive method for the quantitation of microgram quantities of protein utilizing the principle of protein-dye binding. *Anal Biochem* **72:**248–254.

Burns R, Chiueh C, Markey S, Ebert M, Jacobowitz D, and Kopin I (1983) A primate model of parkinsonism: selective destruction of dopaminergic neurons in the pars compacta of the substantia nigra by N-methyl-4-phenyl-1,2,3,6-tetrahydropyridine. *Proc Natl Acad Sci U S A* **80:**4546–4550.

Cadet JL and Brannock C (1998) Free radicals and the pathobiology of brain dopamine systems. *Neurochem Int* **32:**117–131.

Daniels A and Reinhard J, Jr (1988) Energy-driven uptake of the neurotoxin 1-methyl-4-phenylpyridinium into chromaffin granules via the catecholamine transporter. *J Biol Chem* **263:**5034–5036.

Das A, Jeffery JC, Maher JP, McCleverty JA, Schatz E, Ward MD, and Wollermann G (1993) Mono- and binuclear molybdenum and tungsten complexes containing asymmetric bridging ligands: effects of ligand conjugation and conformation on metal-metal interactions. *Inorg Chem* **32:**2145–2155.

Denizot F and Lang R (1986) Rapid colorimetric assay for cell growth and survival: modifications to the tetrazolium dye procedure giving improved sensitivity and reliability. *J Immunol Methods* **89:**271–277.

Di Chiara G, and Imperato A (1988) Drugs abused by humans preferentially increase synaptic dopamine concentrations in the mesolimbic system of freely moving rats. *Proc Natl Acad Sci U S A* **85:**5274–5278.

Frei B, Englan L, and Ames BN (1989) Ascorbate is an outstanding antioxidant in human blood plasma. *Proc Natl Acad Sci U S A* **86:**6377–6381.

Fridovich I (1986) Biological effects of the superoxide radical. *Arch Biochem Biophys* **247:**1–11.

Graham DG (1978) Oxidative pathways for catecholamines in the genesis of neuromelanin and cytotoxic quinones. *Mol Pharmacol* **14:**633–643.

Hald A and Lotharius J (2005) Oxidative stress and inflammation in Parkinson's disease: is there a casual link? *Exp Neurol* **193:**279–290.

Halliwell B (2006) Oxidative stress and neurodegeneration: where are we now? *J Neurochem* **97:**1634–1658.

Kahlig KM, Binda F, Khoshbouei H, Blakely RD, McMahon DG, Javitch JA, and Galli A (2005) Amphetamine induces dopamine efflux through a dopamine transporter channel. *Proc Natl Acad Sci U S A* **102:**3495–3500.

Kahlig KM, Lute BJ, Wei Y, Loland CJ, Gether U, Javitch JA, and Galli A (2006) Regulation of dopamine transporter trafficking by intracellular amphetamine. *Mol Pharmacol* **70:**542–548.

Liu Y, Peter D, Rogahani A, Schuldiner S, Prive GG, Eisenberg D, Brecha N, and Edwards RH (1992) A cDNA that suppresses MPP$^+$ toxicity encodes a vesicular amine transporter. *Cell* **70:**539–551.

Lotharius J and O'Malley KL (2000) The Parkinsonism-inducing drug 1-methyl-4-phenylpyridinium triggers intracellular dopamine oxidation. *J Biol Chem* **275:**38581–38588.

Mattson MP (2006) Neuronal life-and-death signaling, apoptosis, and neurodegenerative disorders. *Antioxid Redox Signal* **8:**1997–2006.

May SW, Mueller PW, Padgette SR, Herman HH, and Phillips RS (1983) Dopamine-?-hydroxylase: suicide inhibition by the novel olefinic substrate, 1-phenyl-1-aminomethylethene. *Biochem Biophys Res Commun* **110:**161–168.

McDonald IA, Lacoste JM, Bey P, Palfreyman MG, and Zreika M (1985) Enzyme-activated irreversible inhibitors of monoamine oxidase: phenylallylamine structure-activity relationships. *J Med Chem* **28:**186–193.

Nair S, Singh SV, and Krishan A (1991) Flow cytometric monitoring of glutathione content and anthracycline retention in tumor cells. *Cytometry* **12:**336–342.

Ogawa N, Asanuma M, Miyazaki I, Diaz-Corrales FJ, and Miyoshi K (2005) L-DOPA treatment from the viewpoint of neuroprotection. Possible mechanism of specific and progressive dopaminergic neuronal death in Parkinson's disease. *J Neurol* **252(Suppl 4):**IV23–IV31.

Oubrahim H, Stadtman ER, and Chock PB (2001) Mitochondria play no roles in Mn(II)-induced apoptosis in HeLa cells. *Proc Natl Acad Sci U S A* **98:**9505–9510.

Padgette SR, Wimalasena K, Herman HH, Sirimanne SR, and May SW (1985) Olefin

oxygenation and *n*-dealkylation by dopamine b-monooxygenase: catalysis and mechanism-based inhibition. *Biochemistry* **24:**5826–5839.

Perera RP, Wimalasena DS, and Wimalasena KW (2003) Characterization of a series of 3-amino-2-phenylpropene derivatives as novel bovine chromaffin vesicular monoamine transporter inhibitors. *J Med Chem* **46:**2599–2605.

Przedborski S, Jackson-Lewis V, Naini AB, Jakowec M, Petzinger G, Miller R, and Akram M (2001) The parkinsonian toxin 1-methyl-4-phenyl-1,2,3,6-tetrahydropyridine (MPTP): a technical review of its utility and safety. *J Neurochem* **76:**1265–1274. P

Riddle EL, Fleckenstein AE, and Hanson GR (2005) Role of monoamine transporters in mediating psychostimulant effects. *AAPS J* **7:**E847–E851.

Rudnick G (1997) Mechanisms of biognic amine transporters, in *Neurotransmitter Transporters: Structure, Function and Regulation* (Reith MEA ed) pp 73–100, Humana Press, Totowa, NJ.

Rudnick G and Wall SC (1992) The molecular mechanism of "Ecstasy" [3,4-methylenedioxymethamphetamine (MDMA)]: serotonin transporters are targets for MDMA-induced serotonin release. *Proc Natl Acad Sci U S A* **89:**1817–1821.

Sabol KE and Seiden LS (1992) Transporters of delight. *Curr Biol* **2:**414–416.

Schuldiner S, Steiner-Mordoch S, Yelin R, Wall SC, and Rudnick G (1993) Amphetamine derivatives interact with both plasma membrane and secretory vesicle biogenic amine transporters. *Mol Pharmacol* **44:**1227–1231.

Smith PK, Krohn RI, Hermanson GT, Mallia AK, Gartner FH, Provenzano MD, Fujimoto EK, Goeke NM, Olson BJ, and Klenk DC (1985) Measurement of protein using bicinchoninic acid. *Anal Biochem* **150:**76–85.

Song X, Perkins S, Jortner BS, and Ehrich M (1997) Cytotoxic effects of MPTP on SH-SY5Y human neuroblastoma cells. *Neurotoxicology* **18:**341–354.

Sulzer D, Bogulavsky J, Larsen KE, Behr G, Karatekin E, Kleinman MH, Turro N, Krantz D, Edwards RH, Greene LA, and Zecca L (2000) Neuromelanin biosynthesis is driven by excess cytosolic catecholamines not accumulated by synaptic vesicles. *Proc Natl Acad Sci U S A* **97:**11869–11874.

Tse DCS, McCreery RL, and Adams RN (1976) Potential oxidative pathways of brain catecholamines. *J Med Chem* **19:**37–40.

Wakefield LM, Cass AEG, and Radda GK (1986) Functional coupling between enzymes of chromaffin granule membrane. *J Biol Chem* **261:**9739–9745.

Watabe M and Nakaki T (2004) Rotenone induces apoptosis via activation of Bad in human dopaminergic SH-SY5Y cells. *J Pharmacol Exp Ther* **311:**948–953.

Wimalasena DS and Wimalasena K (2004) Kinetic evidence for channeling of dopamine between monoamine transporter and membranous dopamine-β-monooxygenase in chromaffin granule ghosts. *J Biol Chem* **279:**15298–15304.

Wimalasena K and Wimalasena DS (1995) The reduction of membrane-bound dopamine β-monooxygenase in resealed chromaffin granule ghosts. Is intragranular ascorbic acid a mediator for extragranular reducing equivalents? *J Biol Chem* **270:**27516–27524.

Address correspondence to: Dr. K. Wimalasena, 1845 N. Fairmount, Department of Chemistry, Wichita State University, Wichita, KS 67260-0051. E-mail: kandatege.wimalasena@wichita.edu